Adaptive Multigrid Methods for Signorini's Problem in Linear Elasticity

Ralf Kornhuber[1] and Rolf Krause[1]

Summary. We derive globally convergent multigrid methods for the discretized Signorini problem in linear elasticity. Special care has to be taken in the case of spatially varying normal directions. In numerical experiments for 2 and 3 space dimensions we observed similar convergence rates as for corresponding linear problems.

1. Introduction.

Contact problems in computational mechanics are of significant importance for a variety of practical applications. Examples are metal forming processes, crash analysis, the design of gear boxes, bearings, car tires or implants in biomechanics. Here, we focus on Signorini's problem in linear elasticity [10, 21, 22, 29] describing the linearized frictionless contact of an elastic body with a rigid foundation. Even in this simple case, the construction of fast, reliable solvers is far from trivial, due to the intrinsic non–differentiable nonlinearity of the problem.

Regularization techniques [7, 11, 13, 14] require careful handling of regularization parameters in order to find a reasonable compromise between efficiency and accuracy. Dual techniques (cf. e.g. [5, 13, 14, 15]) are based on saddle point formulations incorporating the constraints by means of Lagrange multipliers. Active set strategies [2, 16, 18, 20] iteratively provide approximations of the contact set. A linear subproblem with given contact set has to be solved in each iteration step and multigrid methods are typically used for this purpose. An active set strategy with inexact linear solver has been proposed by Dostál [8]. Recently, Schöberl [27, 28] has developed an approximate variant of the projection method (cf. e.g. [13, p. 5]) using a domain decomposition preconditioner and a linear multigrid solver on the interior nodes. Mesh–independent convergence rates are proved, provided that the number of interior nodes is growing with higher order than the number of nodes on the Signorini boundary. Several authors have applied multigrid techniques to scalar obstacle problems directly (see e.g. [4, 6, 12, 16, 19, 23, 26]). Block versions of these methods can be applied in linear elasticity, provided that normal directions are constant along the Signorini boundary. New difficulties arise, as soon as spatially varying normals occur. In this case, the slip conditions at the contact boundary can not be represented on coarse grids.

In this paper we use a direct approach as introduced in [23, 26]. Our algorithm does not involve any regularization or dual formulation and should be considered as a descent method rather than an active set strategy. The basic idea is to minimize the energy on suitably selected d–dimensional subspaces, where $d = 2, 3$ is the dimension of the deformed body. In this way, we obtain nonlinear variants of successive subspace correction methods in the sense of Xu [34]. See e.g. [9, 30] for a similar approach to smooth nonlinear problems. Well–known projected block Gauß–Seidel relaxation is recovered by choosing the d–dimensional subspaces spanned by the fine grid nodal basis functions associated with a fixed node. In order to increase convergence speed by better representation of the low–frequency components of the error, we additionally minimize on subspaces spanned by functions with large support. The suitable selection of these coarse grid spaces is crucial for the efficiency of the resulting method. Our choice is based on sophisticated modifications of the multilevel nodal basis. Straightforward implementation of the resulting algorithm requires additional prolongations in order to check the constraints prescribed on the fine grid. As a consequence, the complexity of one iteration step is $\mathcal{O}(n_\ell \log n_\ell)$ for uniformly refined triangulations and might be even $\mathcal{O}(n_\ell^2)$ in the adaptive case. Optimal complexity of the multigrid V–cycle is recovered by approximating fine grid constraints on coarser grids using so–called *monotone restrictions*. This modification may slow down convergence, as long as the algebraic error is too large. In our numerical experiments we observed that initial iterates as provided by nested iteration are usually accurate enough to provide fast convergence throughout the whole iteration process. Our approach can be extended to more complicated situations like elastic contact or contact with friction. This will be the subject of forthcoming work.

The paper is organized as follows. First we give a brief introduction to Signorini's problem. A general framework for our method including basic convergence results is presented in Section 3. In particular, it turns out that the discrete coincidence set is detected in a finite number of steps, if the given discrete problem is non–degenerate. Then, our nonlinear iteration automatically becomes a linear

[1]Freie Universität Berlin, Fachbereich Mathematik und Informatik, WE 01, Arnimallee 2–6, D-14195 Berlin, Germany

subspace correction method for the resulting linear problem. Hence, asymptotic convergence rates can be obtained by linear multigrid convergence theory. This will the subject of a separate paper.

A suitable multilevel splitting and the monotone restrictions are described in Section 4, respectively. In case of spatially varying normals, various fine grid directions are incorporated in each local coarse grid space. Similar techniques provide appropriate monotone restrictions of fine grid constraints. The resulting *truncated monotone multigrid method* can be arranged as a multigrid V–cycle with projected block Gauß–Seidel smoothing and sophisticated restriction and prolongation. Implementation was carried out in the framework of the finite element toolbox UG [3]. In our numerical experiments to be reported in the final section, we observed mesh independent asymptotic convergence rates. Using nested iteration overall efficiency is similar to the linear selfadjoint case.

2. Signorini's Problem

We consider the deformation of an elastic body as described by the unknown displacement vector $u = (u_1, \dots, u_d)$ defined on the polygonal (polyhedral) reference configuration $\Omega \subset R^d$, $d = 2, 3$. Deformation is caused by volume forces f and traction forces P. We assume that the deformed body is in equilibrium state such that

$$-\sigma_{ij}(u)_{,j} = f_i \qquad \text{in } \Omega. \tag{1}$$

Here and in the following, summation is implicitly taken over indices i, j, s occurring twice and $\sigma_{,j} = \frac{\partial \sigma}{\partial x_j}$ denotes the partial derivative. We further assume that the stress tensor σ is related to the strain tensor ε,

$$\varepsilon_{kl}(u) = \frac{1}{2}(u_{k,l} + u_{l,k}), \quad 1 \le k, l \le d, \tag{2}$$

by Hooke's Law

$$\sigma_{kl}(u) = E_{klij}\varepsilon_{ij}(u), \quad 1 \le i, j, k, l \le d. \tag{3}$$

Hooke's tensor E has the symmetry properties

$$E_{ijkl} = E_{klij} = E_{klji}. \tag{4}$$

The body's surface $\partial\Omega$ is decomposed into three disjoint parts

$$\partial\Omega = \Gamma_D \cup \Gamma_F \cup \Gamma_C$$

with Γ_D having positive measure. We assume that the body is clamped at Γ_D so that

$$u_i = 0 \qquad \text{on } \Gamma_D \tag{5}$$

and traction forces P are applied at Γ_F, giving

$$\sigma_{ij}(u) \cdot \boldsymbol{n}_j = P_i \qquad \text{on } \Gamma_F. \tag{6}$$

Here $\boldsymbol{n} = (n_1, \dots, n_d)$ denotes the outer normal on $\partial\Omega$. The remaining part Γ_C of the body's surface may (or may not) be in contact with a given rigid foundation. Identifying normals on Ω and on the deformed configuration (cf. e.g. [22, p. 19]), we obtain linearized contact conditions

$$\left.\begin{array}{rcl} \sigma_T(u) & = & 0 \\ \sigma_n(u)(u \cdot \boldsymbol{n} - g) & = & 0 \\ u \cdot \boldsymbol{n} - g & \le & 0 \\ \sigma_n(u) & \le & 0 \end{array}\right\} \text{on } \Gamma_C. \tag{7}$$

The function g denotes the initial gap between Ω and the rigid foundation, $\sigma_n = \sigma_{ij} n_i n_j$ and σ_T denote the normal and the tangential component of the stress vector, respectively. Observe that $\sigma_T(u) = 0$ means frictionless contact. We emphasize that the subset of Γ_C where contact actually takes place is not known in advance.

Signorini's problem (cf. [10, 21, 22, 29]) amounts to solve the equilibrium conditions (1) subject to the boundary conditions (5), (6) and (7). Multiplying with a test function v and integrating by parts, Signorini's problem can be reformulated in a weak sense as the variational inequality

$$u \in \mathcal{K}: \qquad a(u, v - u) \ge f(v - u) \qquad \forall v \in \mathcal{K}. \tag{8}$$

Here, the bilinear form

$$a(u, v) = \int_\Omega \sigma_{ij}(u)\, v_{i,j}\, dx$$

is symmetric and elliptic on $H = \{v \in \left(H^1(\Omega)\right)^d \mid v|_{\Gamma_D} = 0\}$. For reasonable data, the functional

$$f(v) = \int_\Omega f_i\, v_i\, dx + \int_{\Gamma_F} P_i\, v_i\, ds\,.$$

is linear and bounded on H. Finally,

$$\mathcal{K} = \{v \in H \mid v \cdot \boldsymbol{n} \leq g \text{ on } \Gamma_C\}$$

denotes the set of admissible displacements. Note that $\mathcal{K}$ is a closed convex subset of H. The variational formulation (8) can be equivalently rewritten as the convex minimization problem

$$u \in \mathcal{K}: \qquad J(u) \leq J(v) \qquad \forall v \in \mathcal{K}, \tag{9}$$

for the quadratic *potential energy functional* $J\colon H \times H \longrightarrow \mathbb{R}$,

$$J(v) = \frac{1}{2}a(v,v) - f(v). \tag{10}$$

Existence and uniqueness of a weak solution u can now be established by direct methods of variational calculus (see e.g. [22, p. 113]).

Let $\mathcal{T}_\ell$ be a given partition of Ω into triangles (tetrahedra) with minimal diameter $h_\ell = \mathcal{O}(2^{-l})$. $\mathcal{N}_\ell$ denotes the set of vertices contained in $\Omega \cup \Gamma_F \cup \Gamma_C$. Discretizing (9) by continuous, piecewise linear finite elements $\mathcal{S}_\ell$,

$$\mathcal{S}_\ell = \{v = (v_1, \ldots, v_d) \in C(\Omega)^d \cap H \;\big|\; v_i|_t \text{ is linear } \forall i = 1, \ldots, d,\ t \in \mathcal{T}_\ell\},$$

we obtain the discrete minimization problem

$$u_\ell \in \mathcal{K}_\ell: \quad J(u_\ell) \leq J(v) \qquad \forall v \in \mathcal{K}_\ell. \tag{11}$$

Here the set $\mathcal{K} \subset H$ is replaced by its discrete analogue $\mathcal{K}_\ell \subset \mathcal{S}_\ell$,

$$\mathcal{K}_\ell = \left\{v \in \mathcal{S}_\ell \mid v(p) \cdot \boldsymbol{n}_\ell(p) \leq g_\ell(p) \quad \forall p \in \mathcal{N}_\ell \cap \Gamma_C\right\}$$

based on suitable approximations $\boldsymbol{n}_\ell$ and g_ℓ of $\boldsymbol{n}$ and g. The subscript ℓ will be mostly skipped in the sequel. Note that in general $\mathcal{K}_\ell \not\subset \mathcal{K}$. Other discretizations, for example by piecewise bilinear functions on quadrilaterals, can be constructed in a similar way.

Of course, (11) admits a unique solution. For shape regular partitions $\mathcal{T}_\ell$ the approximate solutions u_ℓ are converging to u as the meshsize tends to zero. Optimal error estimates in the H^1 norm are available for H^2–regular problems. We refer to [21, pp. 109] or [22, p. 127] for details.

3. Extended Relaxations

The finite element space $\mathcal{S}_\ell$ is spanned by the nodal basis

$$\lambda_p^{(\ell)} \boldsymbol{E}^i, \quad i = 1, \ldots, d, \quad p \in \mathcal{N}_\ell$$

with cartesian unit vectors $\boldsymbol{E}^i \in \mathbb{R}^d$ and piecewise linear, scalar functions $\lambda_p^{(\ell)}$ satisfying

$$\lambda_p^{(\ell)}(q) = \delta_{pq}, \quad p, q \in \mathcal{N}_\ell \qquad \text{(Kronecker delta)}.$$

A nonlinear version of successive subspace correction (cf. Xu [34]) based on the splitting $\mathcal{S}_\ell = V_1 + \ldots + V_{n_\ell}$ with d–dimensional subspaces

$$V_l = \operatorname{span}\{\lambda_{p_l}^{(\ell)} \boldsymbol{E}^1, \ldots, \lambda_{p_l}^{(\ell)} \boldsymbol{E}^d\}, \qquad l = 1, \ldots, n_\ell = \#\mathcal{N}_\ell,$$

gives rise to the well–known projected block Gauß–Seidel relaxation $\mathcal{M}_\ell$ (cf. e.g. [13, p. 151]). As the convergence speed of this method usually deteriorates rapidly with increasing refinement, we consider the *extended splitting*

$$\mathcal{S}_\ell = V_1 + \ldots + V_{n_\ell} + V_{n_\ell+1}^\nu + \ldots + V_m^\nu\,. \tag{12}$$

The additional d–dimensional subspaces V_l^ν, $\nu = n_\ell + 1, \ldots, m$ are intended to improve the representation of low–frequency contributions of the error. Hence, basis functions $\boldsymbol{\mu}_l^{1,\nu}, \ldots, \boldsymbol{\mu}_l^{d,\nu}$ of V_l^ν should have large support. The spaces V_l^ν may vary in each iteration step, in order to allow a stepwise adaptation of the splitting (12) to the coincidence set. The *extended relaxation* based on the extended splitting (12) now reads as follows.

Starting with the given ν–th iterate $u_\ell^\nu = w_0^\nu \in \mathcal{K}_\ell$, we compute a sequence of intermediate iterates $w_l^\nu = w_{l-1}^\nu + v_l^{*,\nu}$, $l = 1, \dots, m$. The new iterate is $u_\ell^\nu = w_m^\nu$. The corrections $v_l^{*,\nu}$ are the unique solutions of the local subproblems

$$v_l^{*,\nu} \in \mathcal{D}_l^{*,\nu} : \quad J(w_{l-1}^\nu + v_l^{*,\nu}) \le J(w_{l-1}^\nu + v) \quad \forall v \in \mathcal{D}_l^{*,\nu}, \tag{13}$$

with closed, convex sets $\mathcal{D}_l^{*,\nu}$ defined by

$$\mathcal{D}_l^{*,\nu} = \{ v \in V_l^\nu \mid w_{l-1}^\nu + v \in \mathcal{K}_\ell \} \subset V_l^\nu. \tag{14}$$

It might be too costly to check whether some $v \in V_l^\nu$ is contained in $\mathcal{D}_l^{*,\nu}$ or not. Hence, optimal corrections $v_l^{*,\nu}$, $l = n_\ell + 1, \dots, m$, are replaced by approximations $v_l^\nu \in V_l^\nu$ provided by approximate local problems

$$v_l^\nu \in \mathcal{D}_l^\nu : \quad J(w_{l-1} + v_l^\nu) \le J(w_{l-1} + v) \quad \forall v \in \mathcal{D}_l^\nu. \tag{15}$$

The closed, convex subsets $\mathcal{D}_l^\nu \subset V_l^\nu$ are intended to approximate $\mathcal{D}_l^{*,\nu}$. They are defined by

$$\mathcal{D}_l^\nu = \{ v \in V_l^\nu \mid v(p_l) \cdot \boldsymbol{e}^i(p_l) \in [\underline{\psi}_l^{i,\nu}, \overline{\psi}_l^{i,\nu}] \ \forall i = 1, \dots, d \}.$$

Here, the local unit vectors $\boldsymbol{e}^i(p_l)$ are obtained by extending $\boldsymbol{e}^1(p_l) = \boldsymbol{n}(p_l)$ to an orthonormal system in $\mathbb{R}^d$, $p_l \in \mathcal{N}_\ell \cap \mathrm{int\ supp}\, \boldsymbol{\mu}_l^{i,\nu}$ and $\underline{\psi}_l^{i,\nu}, \overline{\psi}_l^{i,\nu} \in \mathbb{R}$. We clearly choose $\mathcal{D}_l^\nu = V_l^\nu$ or, equivalently, $\underline{\psi}_l^{i,\nu} = -\infty$, $\overline{\psi}_l^{i,\nu} = +\infty$, if all $v \in V_l^\nu$ satisfy $v|_{\Gamma_C} = 0$. For notational convenience, the index ν will be mostly suppressed in the sequel.

Adapting multigrid terminology, the leading projected block Gauß–Seidel relaxation $\mathcal{M}_\ell$ plays the role of a *fine grid smoother*, $\bar{u}_\ell^\nu = w_{n_\ell}^\nu = \mathcal{M}_\ell(u_\ell^\nu)$ is the *smoothed iterate* and subsequent corrections v_l, $l = n_\ell + 1, \dots, m$ are called *coarse grid corrections.* Note that $\bar{u}_\ell^\nu \in \mathcal{K}_\ell$ holds for all $u_\ell^0 \in \mathcal{S}_\ell$.

THEOREM 1. *Assume that*

$$0 \in \mathcal{D}_l \subset \mathcal{D}_l^*. \tag{16}$$

Then the approximate extended relaxation

$$u_\ell^{\nu+1} = u_\ell^\nu + \sum_{l=1}^{n_\ell} v_l^* + \sum_{l=n_\ell+1}^{m} v_l \tag{17}$$

with v_l^* and v_l computed from (13) and (15), respectively, is globally convergent.

Proof. The sequence of iterates u_ℓ^ν, $\nu = 0, 1, \dots$, is bounded because our scheme (13) is *monotone* in the sense that

$$J(u_\ell^{\nu+1}) \le J(w_{l+1}^\nu) \le J(w_l^\nu) \le J(\bar{u}_\ell^0) < \infty\ , \quad \nu = 1, 2, \dots\ ,$$

and we have $J(v^\nu) \to \infty$ for any unbounded sequence $v^\nu \in \mathcal{S}_\ell$.

As u_ℓ^ν is bounded and $\mathcal{S}_\ell$ has finite dimension, it is sufficient to show that each convergent subsequence of u_ℓ^ν converges to u_ℓ. Let $u_\ell^{\nu_k}$ be an arbitrary, convergent subsequence of u_ℓ^ν, with some limit $u^* \in \mathcal{S}_\ell$,

$$u_\ell^{\nu_k} \to u^*, \quad k \to \infty. \tag{18}$$

It is easily checked that $\mathcal{M}_\ell$ is continuous so that

$$\mathcal{M}_\ell(u_\ell^{\nu_k}) \to \mathcal{M}_\ell(u^*), \quad k \to \infty. \tag{19}$$

Again, monotonicity of the iteration implies

$$J(u_\ell^{\nu_{k+1}}) \le J(u_\ell^{\nu_k + 1}) \le J(\mathcal{M}_\ell(u_\ell^{\nu_k})) \le J(u_\ell^{\nu_k}).$$

In virtue of the convergence (18), (19) and the continuity of J on $\mathcal{K}_\ell$, this leads to

$$J(\mathcal{M}_\ell(u^*)) = J(u^*). \tag{20}$$

It is easily seen that (20) holds, if and only if all local corrections of the projected block Gauß–Seidel relaxation applied to u^* are zero, i.e., $\mathcal{M}_\ell(u^*) = u^*$. As the finite element solution u_ℓ is the only fixed point of the projected block Gauß–Seidel relaxation (cf. e.g. [13, p. 152]), we have shown $u^* = u_\ell$. This completes the proof. □

As a corollary, we also obtain convergence of the intermediate iterates

$$w_l^\nu \to u_\ell \qquad \nu \to \infty. \tag{21}$$

Indeed, the sequence w_l^ν, $\nu = 0, 1, \dots$, is bounded and due to the monotonicity

$$J(u_\ell^{\nu_k + 1}) \le J(w_l^{\nu_k}) \le J(u_\ell^{\nu_k})$$

and the continuity of J on $\mathcal{K}_\ell$ the limit w^* of an arbitrary convergent subsequence $w_l^{\nu_k}$, $k = 0, 1, \ldots$, must satisfy $J(w^*) = J(u_\ell)$, giving $w^* = u_\ell$.

For given $w \in \mathcal{K}_\ell$, we define the *discrete coincidence set*

$$\mathcal{N}_\ell^\bullet(w) = \{p \in \mathcal{N}_\ell \cap \Gamma_C \mid w(p) \cdot \boldsymbol{n}(p) = g(p)\}.$$

No contact occurs at $\mathcal{N}_\ell^\circ(w) = \mathcal{N}_\ell \backslash \mathcal{N}_\ell^\bullet(w)$. Once the coincidence set $\mathcal{N}_\ell^\bullet(u_\ell)$ is known, the minimization problem (11) can be rewritten as the *reduced linear problem*

$$a(u_\ell, v) = f(v) \qquad \forall v \in \mathcal{S}_\ell^\circ \tag{22}$$

where the subspace $\mathcal{S}_\ell^\circ \subset \mathcal{S}_\ell$ is defined by

$$\mathcal{S}_\ell^\circ = \{v \in \mathcal{S}_\ell \mid v(p) \cdot \boldsymbol{n}(p) = 0 \ \ \forall p \in \mathcal{N}_\ell^\bullet(u_\ell)\}.$$

In the remainder of this section, we will show that the iteration (17) is asymptotically reducing to a linear subspace correction method for the linear problem (22).

LEMMA 1. *Assume that the discrete problem (11) is non–degenerate in the sense that*

$$f(\lambda_p^{(\ell)} \boldsymbol{n}(p)) - a(u_\ell, \lambda_p^{(\ell)} \boldsymbol{n}(p)) > 0 \qquad \forall p \in \mathcal{N}_\ell^\bullet(u_\ell) \tag{23}$$

and that the coarse grid spaces V_l^ν in (12) are chosen such that

$$\boldsymbol{\mu}_l^{i,\nu}(p) \cdot \boldsymbol{n}(p) = 0 \qquad \forall p \in \mathcal{N}_\ell^\bullet(\bar{u}_\ell^\nu) \tag{24}$$

holds for all $\nu \geq 0$.

Then there is a $\nu_0 \geq 0$ such that

$$\mathcal{N}_\ell^\bullet(u_\ell^\nu) = \mathcal{N}_\ell^\bullet(u_\ell) \qquad \forall \nu \geq \nu_0. \tag{25}$$

Proof. Let $p \in \mathcal{N}_\ell^\circ(u_\ell) \cap \Gamma_C$ or, equivalently, $u_\ell(p) \cdot \boldsymbol{n}(p) < g(p)$. Convergence of u_ℓ^ν implies $u_\ell^\nu(p) \cdot \boldsymbol{n}(p) < g(p)$ $\forall \nu \geq \nu_0$ with sufficiently large ν_0. Hence,

$$\mathcal{N}_\ell^\circ(u_\ell) \subset \mathcal{N}_\ell^\circ(u_l^\nu) \qquad \forall \nu \geq \nu_0.$$

Now, let $p_l \in \mathcal{N}_\ell^\bullet(u_\ell)$. As a consequence of (23) and of convergence of intermediate iterates (21), we obtain

$$f(\lambda_{p_l}^{(\ell)} \boldsymbol{n}(p_l)) - a(w_l^\nu, \lambda_{p_l}^{(\ell)} \boldsymbol{n}(p_l)) > 0 \qquad \forall \nu \geq \nu_0 \tag{26}$$

for $l = 1, \ldots, n_\ell$ and sufficiently large ν_0. Now assume that $p_l \notin \mathcal{N}_\ell^\bullet(\bar{u}_\ell^\nu)$ or, equivalently,

$$\bar{u}_\ell^\nu(p_l) \cdot \boldsymbol{n}(p_l) = w_{l-1}^\nu(p_l) \cdot \boldsymbol{n}(p_l) + v_l^{*,\nu}(p_l) \cdot \boldsymbol{n}(p_l) < g(p_l).$$

In the light of (13), the correction $v_l^{*,\nu}$ then satisfies the variational equality

$$a(v_l^{*,\nu}, v) = f(v) - a(w_{l-1}^\nu, v) \qquad \forall v \in V_l.$$

Hence, $f(v) - a(w_l^\nu, v) = 0$ $\forall v \in V_l$ in contradiction to (26). We have shown

$$\mathcal{N}_\ell^\bullet(u_\ell) \subset \mathcal{N}_\ell^\bullet(\bar{u}_\ell^\nu) \qquad \forall \nu \geq \nu_0.$$

It is clear from (24) that $\mathcal{N}_\ell^\bullet(\bar{u}_\ell^\nu) \subset \mathcal{N}_\ell^\bullet(u_\ell^{\nu+1})$, giving $\mathcal{N}_\ell^\bullet(u_\ell) \subset \mathcal{N}_\ell^\bullet(u_\ell^\nu)$ $\forall \nu \geq \nu_0 + 1$. This completes the proof. $\square$

As a by–product of the proof, we also get

$$\mathcal{N}_\ell^\bullet(\bar{u}_\ell^\nu) = \mathcal{N}_\ell^\bullet(u_\ell) \qquad \nu \geq \nu_0. \tag{27}$$

Observe that condition (24) guarantees that corrections in the direction of $\boldsymbol{\mu}_l^{i,\nu}$ do not affect the actual guess of the coincidence set $\mathcal{N}_\ell^\bullet(\bar{u}_\ell^\nu)$. As a consequence of (24) coarse grid correction asymptotically reduces to linear subspace correction for the reduced problem (22) provided that no constraints are active. This can be ensured by appropriate choice of local obstacles $\underline{\psi}_l^{i,\nu}$, $\overline{\psi}_l^{i,\nu}$.

Assume that V_l^ν solely depends on $\mathcal{N}_\ell^\bullet(\bar{u}_\ell^\nu)$, i.e., $V_l^\nu = V_l(\mathcal{N}_\ell^\bullet(\bar{u}_\ell^\nu))$. Then, a sequence of local obstacles $\underline{\psi}_l^{i,\nu}$, $\overline{\psi}_l^{i,\nu}$, $\nu \geq 0$, is called *quasioptimal* (cf. [23]), if convergence of the intermediate iterates w_l^ν (see (21)) and convergence of the coincidence sets $\mathcal{N}_\ell^\bullet(\bar{u}_\ell^\nu)$ (see (27)) implies that there is a positive number ψ^*, independent of ν, and some $\nu_0 \geq 0$, such that

$$\underline{\psi}_l^{i,\nu} \leq -\psi^* < 0 < \psi^* \leq \overline{\psi}_l^{i,\nu} \qquad \forall \nu \geq \nu_0. \tag{28}$$

holds for all $i = 1, \ldots, d$ and $l = n_\ell + 1, \ldots, m$.

THEOREM 2. *Assume that the assumptions of Lemma 1 are satisfied. Assume further that the coarse grid spaces only depend on the actual guess of the coincidence set, i.e.,* $V_l^\nu = V_l(\mathcal{N}_\ell^\bullet(\bar{u}_\ell^\nu))$*, and that the local obstacles* $\underline{\psi}_l^i$*,* $\overline{\psi}_l^i$ *are quasioptimal in the sense of (28).*

Then there is a $\nu_0 > 0$ *such that the approximate extended relaxation (17) is reducing to the linear successive subspace correction induced by the splitting*

$$\mathcal{S}_\ell{}^\circ = V_1^\circ + \cdots + V_m^\circ$$

with

$$V_l^\circ = \begin{cases} V_l \cap \mathcal{S}_\ell{}^\circ, & l = 1, \ldots, n_\ell \\ V_l(\mathcal{N}_\ell{}^\bullet(u_\ell)), & l = n_\ell + 1 \ldots, m \end{cases}$$

as applied to the reduced linear problem (22).

Proof. Let $l = 1, \ldots, n_\ell$. There is nothing to show, if $p_l \notin \Gamma_C$. Let $p_l \in \mathcal{N}_\ell{}^\bullet(u_\ell)$. As a consequence of Lemma 1 and (27), the normal components of $v_l^{*,\nu}$ are zero, if ν is sufficiently large. In this case, we have $v_l^{*,\nu} \in V_l \cap \mathcal{S}_\ell{}^\circ = V_l^\circ$ and $V_l^\circ = \mathcal{D}_l{}^{*,\nu}$ so that

$$J(w_{l-1} + v_l^{*,\nu}) \le J(w_{l-1} + v) \qquad \forall v \in V_l^\circ. \tag{29}$$

In the remaining case $p_l \in \mathcal{N}_\ell{}^\circ(u_\ell) \cap \Gamma_C$ it follows directly from (27) that $v_l^{*,\nu}$ must satisfy (29) with $V_l^\circ = V_l$ for sufficiently large ν.

Now, let $l = n_\ell + 1, \ldots, m$. Then, exploiting (27) we get $V_l^\nu = V_l(\mathcal{N}_\ell{}^\bullet(u_\ell))$, i.e., $V_l^\nu = V_l^\circ$, for sufficiently large ν. Convergence of the intermediate iterates w_l^ν (21) implies that the corrections v_l^ν must tend to zero. Utilizing (28), it follows that

$$v_l^\nu(p_l) \cdot \boldsymbol{e}^i(p_l) \in [-\psi^*, \psi^*] \subset (\underline{\psi}_l^{i,\nu}, \overline{\psi}_l^{i,\nu})$$

holds for sufficiently large ν. In this case,

$$J(w_{l-1} + v_l^\nu) \le J(w_{l-1} + v) \qquad \forall v \in V_l^\circ$$

and the assertion follows. □

Using optimal corrections from (13) instead of quasioptimal approximations (cf. Theorem 2), we asymptotically get the same linear subspace correction method for (22).

4. Truncated Monotone Multigrid Methods.

Assume that $\mathcal{T}_\ell$ is resulting from ℓ refinements of an intentionally coarse triangulation $\mathcal{T}_0$. Though the algorithms and convergence results to be presented can be easily generalized to the non–uniform case, let us assume for the moment that the triangulations are uniformly refined. More precisely, each triangle $t \in \mathcal{T}_k$ is subdivided into four congruent subtriangles in order to produce the next triangulation $\mathcal{T}_{k+1}$.

Using this hierarchy of grids and the corresponding hierarchy of finite element spaces, we now choose suitable spaces $V_{n_\ell+1}, \ldots, V_m$. Each space $V_l = V_{l(p,k)}$ is associated with a node $p \in \mathcal{N}_k$ on some refinement level $k \le \ell - 1$. We frequently use the notation $V_p^{(k)} = V_{l(p,k)}$, $\boldsymbol{\mu}_p^{(k)} = \boldsymbol{\mu}_{l(p,k)}$, etc. The ordering $l = l(p,k)$ is taken from fine to coarse, i.e., $l(p,k) \le l(q,j)$ implies $k \ge j$.

For each $p \in \mathcal{N}_\ell$ we choose a local orthonormal system $\boldsymbol{e}^i(p) \in \mathbb{R}^d$, $i = 1, \ldots d$, with the property $\boldsymbol{e}^1(p) = \boldsymbol{n}(p)\ \forall p \in \mathcal{N}_\ell \cap \Gamma_C$. Starting with

$$\left(\boldsymbol{\mu}_p^{(\ell)}\right)^i = \begin{cases} 0 & \text{if } i = 1 \text{ and } p \in \mathcal{N}_\ell{}^\bullet(\bar{u}_\ell^\nu) \\ \lambda_p^{(\ell)} \boldsymbol{e}^i(p) & \text{else} \end{cases}, \tag{30}$$

we recursively define truncated basis functions

$$\left(\boldsymbol{\mu}_p^{(k-1)}\right)^i = \sum_{q \in \mathcal{N}_k} \lambda_p^{(k-1)}(q)\ \boldsymbol{e}^i(p) \cdot \boldsymbol{e}^j(q)\ \left(\boldsymbol{\mu}_q^{(k)}\right)^j \tag{31}$$

(summation over j) and we set

$$V_p^{(k)} = \operatorname{span}\{\left(\boldsymbol{\mu}_p^{(k)}\right)^1, \ldots, \left(\boldsymbol{\mu}_p^{(k)}\right)^d\} \qquad k = \ell - 1, \ldots, 0. \tag{32}$$

Note that supp $\left(\boldsymbol{\mu}_p^{(k)}\right)^i =$ supp $\lambda_p^{(k)}$ and $\left(V_p^{(k)}\right)^\nu = V_p^{(k)}(\mathcal{N}_\ell{}^\bullet(\bar{u}_\ell^\nu))$ only depends on $\mathcal{N}_\ell{}^\bullet(\bar{u}_\ell^\nu)$.

LEMMA 2. *Let* $0 \le k \le \ell$*,* $p \in \mathcal{N}_k$ *and* $1 \le i, j \le d$*. Then*

$$\left(\boldsymbol{\mu}_p^{(k)}\right)^i(q) \cdot \boldsymbol{e}^j(q) = \begin{cases} 0 & \text{if } j = 1 \text{ and } q \in \mathcal{N}_\ell{}^\bullet(\bar{u}_\ell^\nu) \\ \lambda_p^{(k)}(q)\ \boldsymbol{e}^i(p) \cdot \boldsymbol{e}^j(q) & \text{else} \end{cases} \tag{33}$$

holds for all $q \in \mathcal{N}_\ell$*.*

Proof. The assertion is clear for $k=\ell$. Assume that (33) holds for some $k \le \ell$. If $j \neq 1$ or $q \notin \mathcal{N}_\ell^\bullet(\bar{u}_\ell^\nu)$ we obtain (summation on s)

$$\begin{aligned}
\left(\boldsymbol{\mu}_p^{(k-1)}\right)^i(q)\cdot \boldsymbol{e}^j(q) &= \sum_{r\in\mathcal{N}_k} \lambda_p^{(k-1)}(r)\; \boldsymbol{e}^i(p)\cdot \boldsymbol{e}^s(r)\; \left(\boldsymbol{\mu}_r^{(k)}\right)^s(q)\cdot \boldsymbol{e}^j(q)\\
&= \sum_{r\in\mathcal{N}_k} \lambda_p^{(k-1)}(r)\; \lambda_r^{(k)}(q)\; \boldsymbol{e}^i(p)\cdot \boldsymbol{e}^s(r)\; \boldsymbol{e}^s(r)\cdot \boldsymbol{e}^j(q)\\
&= \sum_{r\in\mathcal{N}_k} \lambda_p^{(k-1)}(r)\; \lambda_r^{(k)}(q)\; \boldsymbol{e}^i(p)\cdot \boldsymbol{e}^j(q)\\
&= \lambda_p^{(k-1)}(q)\; \boldsymbol{e}^i(p)\cdot \boldsymbol{e}^j(q)
\end{aligned}$$

exploiting the identity

$$\boldsymbol{e}^i(p)\cdot \boldsymbol{e}^s(r)\; \boldsymbol{e}^s(r)\cdot \boldsymbol{e}^j(q) = \boldsymbol{e}^i(p)\cdot \boldsymbol{e}^j(q) \qquad p,q,r\in\mathcal{N}_\ell.$$

Now let $q \in \mathcal{N}_\ell^\bullet(\bar{u}_\ell^\nu)$. Then definition (30) yields

$$\left(\boldsymbol{\mu}_p^{(\ell)}\right)^i(q)\cdot \boldsymbol{n}(q) = 0 \qquad \forall i=1,\dots,d,\;\; p\in\mathcal{N}_\ell.$$

Using (31) the assertion now follows by induction. □

Lemma 2 reveals the construction principle of coarse grid spaces $V_p^{(k)}$. If $q \notin \mathcal{N}_\ell^\bullet(\bar{u}_\ell^\nu)$, we get

$$\left(\boldsymbol{\mu}_p^{(k)}\right)^i(q) = \lambda_p^{(k)}(q)\; \boldsymbol{e}^i(p) \qquad \forall i=1,\dots,d.$$

Hence, $V_p^{(k)} = \operatorname{span}\{\lambda_p^{(k)}\boldsymbol{E}^1,\dots,\lambda_p^{(k)}\boldsymbol{E}^d\}$, if there is no contact in the neighborhood of p or, more precisely, if int supp $\lambda_p^{(k)} \cap \mathcal{N}_\ell^\bullet(\bar{u}_\ell^\nu) = \emptyset$. In this case, we obtain the same local correction $v_p^{(k)}$ as classical multigrid method with canonical Galerkin restriction and block Gauß–Seidel smoother. On the other hand, if $q\in\mathcal{N}_\ell^\bullet(\bar{u}_\ell^\nu)$, Lemma 2 provides

$$\left(\boldsymbol{\mu}_p^{(k)}\right)^i(q)\cdot \boldsymbol{n}(q) = 0 \qquad \forall i=1,\dots,d.$$

Hence, the spaces $V_p^{(k)}$ satisfy condition (24).

Roughly speaking, coarse grid basis functions $\left(\boldsymbol{\mu}_p^{(k)}\right)^i$ are obtained by careful truncation and bending of nodal basis functions $\lambda_p^{(k)}\boldsymbol{e}^i(p)$. In case of constant normal directions, i.e., $\boldsymbol{e}^i(p)=\boldsymbol{e}^i(q)$ $\forall p,q\in\mathcal{N}_\ell$, (31) reduces to canonical restriction

$$\left(\boldsymbol{\mu}_p^{(k-1)}\right)^i = \sum_{q\in\mathcal{N}_k} \lambda_p^{(k-1)}(q)\; \left(\boldsymbol{\mu}_q^{(k)}\right)^i. \tag{34}$$

Note that canonical restriction (34) could be used in the case of spatially varying normals as well, because the resulting coarse grid basis functions would still satisfy (24). However, varying normals cause large energy of such coarse grid functions which leads to poor convergence rates of the corresponding subspace correction. Similar effects caused by jumping coefficients have been investigated e.g. by Wan et al. [31].

In order to complete the construction of our multigrid method, we now describe the recursive construction of local obstacles $\underline{\psi}^i_{l(p,k)} = (\underline{\psi}_p^{(k)})^i$, $\overline{\psi}^i_{l(p,k)} = (\overline{\psi}_p^{(k)})^i$, $k=\ell-1,\dots,0$, occurring in (14). Starting with

$$\begin{array}{llllll}
\left(\underline{\psi}_p^{(\ell)}\right)^1 = -\infty, & \left(\overline{\psi}_p^{(\ell)}\right)^1 = g(p) - \bar{u}_\ell^\nu(p)\cdot \boldsymbol{n}(p) & & \\
\left(\underline{\psi}_p^{(\ell)}\right)^i = -\infty & \left(\overline{\psi}_p^{(\ell)}\right)^i = +\infty & i=2,\dots,d & p\in\mathcal{N}_\ell,
\end{array} \tag{35}$$

we assume that local obstacles $(\underline{\psi}_p^{(k)})^i$, $(\overline{\psi}_p^{(k)})^i$ have been constructed for some $k\le\ell$. For fixed $p\in\mathcal{N}_{k-1}$ and $i=1,\dots d$ local obstacles on the next coarser level are now obtained by *monotone restriction* defined as follows

$$(\underline{\psi}_p^{(k-1)})^i = d_i^{-1}\max(\Psi_p^i)_-\,, \qquad (\overline{\psi}_p^{(k-1)})^i = d_i^{-1}\min(\Psi_p^i)_+\,. \tag{36}$$

The factor $d_i \le d$ denotes the number of non–zero entries in the i–th row of $\big(\boldsymbol{e}^i(p)\cdot\boldsymbol{e}^j(q)\big)_{i,j=1,\dots d}$. Further let

$$\Psi_p^i = \left\{ \frac{(\underline{\psi}_q^{(k)})^j}{\boldsymbol{e}^i(p)\cdot\boldsymbol{e}^j(q)}, \frac{(\overline{\psi}_q^{(k)})^j}{\boldsymbol{e}^i(p)\cdot\boldsymbol{e}^j(q)} \;\Big|\; q \in \text{int supp } \lambda_p^{(k-1)} \cap \mathcal{N}_k,\ j=1,\dots,d,\right.$$
$$\left. j \neq 1 \text{ or } q \notin \mathcal{N}_\ell^\bullet(\bar{u}_\ell^\nu),\ \boldsymbol{e}^i(p)\cdot\boldsymbol{e}^j(q) \neq 0 \right\}.$$

The sets $(\Psi_p^i)_-$ and $(\Psi_p^i)_+$ contain the nonpositive and nonnegative elements of Ψ_p^i, respectively. Observe that the weights $\boldsymbol{e}^i(p)\cdot\boldsymbol{e}^j(q)$ may be positive, negative or zero.

Once all local corrections $v_p^{(k-1)} = v_{l(p,k)}$ on level $k-1$ have been computed from (15), we update the obstacles according to

$$\begin{aligned} \big(\underline{\psi}_p^{(k-1)}\big)^i &\to \big(\underline{\psi}_p^{(k-1)}\big)^i - v_p^{(k-1)}(p)\cdot\boldsymbol{e}^i(p) \\ \big(\overline{\psi}_p^{(k-1)}\big)^i &\to \big(\overline{\psi}_p^{(k-1)}\big)^i - v_p^{(k-1)}(p)\cdot\boldsymbol{e}^i(p) \end{aligned} \qquad p \in \mathcal{N}_{k-1}. \tag{37}$$

Monotone restriction (36) and update (37), are repeated inductively until the coarsest level $k=0$ is reached. It is clear by construction that

$$(\underline{\psi}_p^{(k)})^i \le 0 \le (\underline{\psi}_p^{(k)})^i \qquad k=\ell-1,\dots,0. \tag{38}$$

Lemma 3. *Let $\bar{u}_\ell^\nu \in \mathcal{K}_\ell$. Then the subsets $\mathcal{D}_l = \mathcal{D}_p^{(k)}$,*

$$\mathcal{D}_p^{(k)} = \{v \in V_p^{(k)} \mid v(p)\cdot\boldsymbol{e}^i(p) \in [(\underline{\psi}_p^{(k)})^i, (\overline{\psi}_p^{(k)})^i]\ \forall i=1,\dots,d\}$$

satisfy condition (16).

Proof. From corrections on levels ℓ to $k \le \ell$ we obtain the intermediate iterate $w^{(k)}$,

$$w^{(k)} = u_\ell^\nu + \sum_{j=k}^{\ell}\sum_{p\in\mathcal{N}_j} v_p^{(k)}.$$

We show by induction that

$$w^{(k)} + \sum_{p\in\mathcal{N}_{k-1}} z_p^{(k-1)} \in \mathcal{K}_\ell \qquad \forall z_p^{(k-1)} \in \mathcal{D}_p^{(k-1)}, \qquad k=\ell,\dots,1, \tag{39}$$

holds after monotone restriction (36). Simultaneously, we prove the auxiliary result

$$w^{(k)} + \sum_{p\in\mathcal{N}_k} z_p^{(k)} \in \mathcal{K}_\ell \qquad \forall z_p^{(k)} \in \mathcal{D}_p^{(k)}, \qquad k=\ell,\dots,0, \tag{40}$$

where $\mathcal{D}_p^{(k)}$ is taken after update (37) for $k=\ell-1,\dots,0$.

Assertion (40) is clear for $k=\ell$. Assuming that (40) holds for some $k=\ell,\dots,1$ we now prove (39). Let $z_p^{(k-1)} = (z_p^{(k-1)})_i\ (\boldsymbol{\mu}_p^{(k-1)})^i \in \mathcal{D}_p^{(k-1)}$. Inserting (31), we get the representation

$$\sum_{p\in\mathcal{N}_{k-1}} z_p^{(k-1)} = \sum_{p\in\mathcal{N}_k} z_p^{(k)}$$

with

$$z_p^{(k)} = \sum_{q\in\mathcal{N}_{k-1}} \lambda_q^{(k-1)}(p)\ (z_q^{(k-1)})_i\ \boldsymbol{e}^i(q)\cdot\boldsymbol{e}^j(p)\ \big(\boldsymbol{\mu}_p^{(k)}\big)^j \in V_p^{(k)}.$$

Let $j \neq 1$ or $p \notin \mathcal{N}_\ell^\bullet(\bar{u}_\ell^\nu)$. Exploiting (36), we get

$$z_p^{(k)}(p)\cdot\boldsymbol{e}^j(p) = \sum_{q\in\mathcal{N}_{k-1}} \lambda_q^{(k-1)}(p)\ (z_p^{(k-1)})_i\ \boldsymbol{e}^i(q)\cdot\boldsymbol{e}^j(p) \in [(\underline{\psi}_p^{(k)})^j, (\overline{\psi}_p^{(k)})^j]$$

for all $j=1,\dots,d$. In the remaining case, $j=1$ and $p \in \mathcal{N}_\ell^\bullet(\bar{u}_\ell^\nu)$, Lemma 2 leads to

$$z_p^{(k)}(p)\cdot\boldsymbol{e}^1(p) = 0 \in \big[(\underline{\psi}_p^{(k)})^1, (\overline{\psi}_p^{(k)})^1\big].$$

Hence, $z_p^{(k)} \in \mathcal{D}_p^{(k)}\ \forall p \in \mathcal{N}_k$ and (39) follows from (40).

Finally, it is easily seen that the update (37) is performed in such a way that (40) holds for $k-1$. $\square$

LEMMA 4. *The local obstacles* $\underline{\psi}^i_{l(p,k)} = (\underline{\psi}^{(k)}_p)^i$, $\overline{\psi}^i_{l(p,k)} = (\overline{\psi}^{(k)}_p)^i$, $k = \ell-1,\dots,0$, *as obtained from (36) and (37) are quasioptimal in the sense of (28).*

Proof. The local obstacles as obtained from (36) and (37) depend continuously on the smoothed iterate $\bar{u}^\nu_\ell$ and on the coarse grid corrections $v^{(k)}_p$. As $\bar{u}^\nu_\ell \to u_\ell$ and $v^{(k)}_p \to 0$, it is sufficient to show that (28) holds if $\bar{u}^\nu_\ell$ and $v^{(k-1)}_p$ are replaced by u_ℓ and 0, respectively. This can be done by induction. □

In case of constant normal directions, i.e., $\boldsymbol{e}^i(p) = \boldsymbol{e}^i(q)\ \forall p,q \in \mathcal{N}_\ell$, definition (36) reduces to the restriction

$$\left(\overline{\psi}^{(k-1)}_p\right)^1 = \min\left\{ \left(\overline{\psi}^{(k)}_q\right)^1 \mid q \in (\text{int supp } \lambda^{(k-1)}_p \cap \mathcal{N}_k) \setminus \mathcal{N}_\ell^\bullet(\bar{u}^\nu_\ell)\right\}$$

as proposed by Mandel [26] in the scalar case (see also [23]). No tangential constraints occur on coarse grids. However, in case of spatially varying normal directions monotone restriction (36) causes tangential constraints on coarse levels though no such constraints are present on the finest grid. This leads to more pessimistic coarse grid constraints in comparison with the scalar case. Improvements of (36) are possible by generalizing ideas from [23].

Now we are ready to state the main result of this section.

THEOREM 3. *The truncated monotone multigrid method based on local spaces* $V^{(k)}_p$ *from (32) and on local obstacles* $\underline{\psi}^{(k)}_p$, $\overline{\psi}^{(k)}_p$ *as obtained from (36) and (37) is globally convergent. If the discrete problem (11) satisfies the non–degeneracy condition (23), then there is a* $\nu_0 \geq 0$ *such that the iteration reduces to the linear subspace correction method for the linear reduced problem (22) induced by the splitting*

$$\mathcal{S}_\ell{}^\circ = \sum_{k=0}^{\ell} \sum_{p\in\mathcal{N}_k} \left(V^{(k)}_p\right)^\circ \tag{41}$$

with $\left(V^{(\ell)}_p\right)^\circ = V^{(\ell)}_p \cap \mathcal{S}_\ell{}^\circ$, $p \in \mathcal{N}_\ell$, *and* $\left(V^{(k)}_p\right)^\circ = V^{(k)}_p(\mathcal{N}_\ell{}^\bullet(u_\ell))$, $p \in \mathcal{N}_k$, $k = \ell-1,\dots,0$.

Proof. Utilizing (38) and Lemma 3, global convergence follows from Theorem 1. Asymptotic reduction to a linear iteration follows from Theorem 2 in combination with Lemma 3 and Lemma 4. □

Note that splitting (41) depends only on the choice of additional coarse grid spaces and not on the choice of quasioptimal restriction. In the light of Theorem 3 linear multigrid convergence theory can be applied in order to derive asymptotic convergence rates. This will the subject of a forthcoming paper.

5. IMPLEMENTATION

We shall derive an algebraic reformulation of the truncated monotone multigrid method considered in Theorem 3. The resulting algorithm can be implemented as a usual multigrid V–cycle. Denoting

$$\boldsymbol{a}_{pq} = \left(a(\lambda^{(\ell)}_p \boldsymbol{e}^i, \lambda^{(\ell)}_q \boldsymbol{e}^j)\right)_{i,j=1,\dots,d}, \qquad \boldsymbol{b}_p = \left(f(\lambda^{(\ell)}_p \boldsymbol{e}^i)\right)_{i=1,\dots,d}$$

we define the stiffness matrix and right hand side

$$\boldsymbol{A} = (\boldsymbol{a}_{pq})_{p,q\in\mathcal{N}_\ell}, \qquad \boldsymbol{b} = (b_p)_{p\in\mathcal{N}_\ell}.$$

The vector representation of the given iterate u^ν_ℓ is

$$\boldsymbol{u}^\nu_\ell = (\boldsymbol{u}_p)_{p\in\mathcal{N}_\ell}, \qquad \boldsymbol{u}_p = (u^i_p)_{i=1,\dots,d}, \qquad u^i_p = u^\nu_\ell(p)\cdot \boldsymbol{e}^i(p). \tag{42}$$

We shall use a similar partitioning of vectors $\boldsymbol{v} = (v^i_p)_{p\in\mathcal{N}_k, i=1,\dots,d} \in \mathbb{R}^{dn_k}$ on all levels $0 \leq k \leq \ell$. The residual is given by

$$\boldsymbol{r} = \boldsymbol{b} - \boldsymbol{A}\boldsymbol{u}^\nu_\ell.$$

Solving the defect problem

$$\boldsymbol{v}^* \in \boldsymbol{\mathcal{D}}: \qquad \tfrac{1}{2}\boldsymbol{v}^*\cdot\boldsymbol{A}\boldsymbol{v}^* - \boldsymbol{r}\cdot\boldsymbol{v}^* \leq \tfrac{1}{2}\boldsymbol{v}\cdot\boldsymbol{A}\boldsymbol{v} - \boldsymbol{r}\cdot\boldsymbol{v} \qquad \forall \boldsymbol{v}\in\boldsymbol{\mathcal{D}} \tag{43}$$

with constraints

$$\boldsymbol{\mathcal{D}} = \{\boldsymbol{v}\in\mathbb{R}^{dn_\ell} \mid v^1_p \leq g(p) - u^1_p\ \forall p \in \mathcal{N}_\ell \cap \Gamma_C\}$$

exactly, we would obtain the exact solution $\boldsymbol{u}_\ell = \boldsymbol{u}^\nu_\ell + \boldsymbol{v}^*$. The approximate correction as obtained by one step of projected block Gauß–Seidel relaxation with $d\times d$ blocks $\boldsymbol{a}_{pq}$ is denoted by $GS_\ell(\boldsymbol{A},\boldsymbol{r},\boldsymbol{\mathcal{D}})$. Hence, vector representation of the smoothed iterate $\bar{u}^\nu_\ell$ is given by

$$\bar{\boldsymbol{u}}^\nu_\ell = \boldsymbol{u}^\nu_\ell + GS_\ell(\boldsymbol{A},\boldsymbol{r},\boldsymbol{\mathcal{D}}).$$

Now, we describe the coarse grid correction of $\bar{\boldsymbol{u}}_\ell^\nu$. It is clear how to obtain the actual coincidence set $\mathcal{N}_\ell^\bullet(\bar{u}_\ell^\nu)$. We define the truncated stiffness matrix $\boldsymbol{A}^{(\ell)} = \mathrm{trc}(\boldsymbol{A})$ by setting those rows and columns of $\boldsymbol{A}$ to zero that are associated with basis functions $\lambda_p \boldsymbol{e}^1(p)$, $p \in \mathcal{N}_\ell^\bullet(\bar{u}_\ell^\nu)$. In practical implementation this is realized by appropriate flags. Using the partitioning $\boldsymbol{v} = (v_p^i)_{p\in\mathcal{N}_k, i=1,\dots,d}$ of some vector $\boldsymbol{v} \in \mathbb{R}^{dn_k}$ on some level k, the vector $\mathrm{trc}(v)$ is obtained by annihilating all v_p^1 with $p \in \mathcal{N}_\ell^\bullet(\bar{u}_\ell^\nu) \cap \mathcal{N}_k$. The truncated residual is given by $\boldsymbol{r}^\ell = \mathrm{trc}(\boldsymbol{b} - \boldsymbol{A}\bar{\boldsymbol{u}}_\ell^\nu)$.

Recursive definition (31) of $\boldsymbol{\mu}_p^{(k)}$ gives rise to the restriction matrix $\boldsymbol{R}_k^{k-1}$,

$$\boldsymbol{R}_k^{k-1} = (\lambda_p^{(k)}(q)\boldsymbol{e}_{pq})_{p\in\mathcal{N}_{k-1}, q\in\mathcal{N}_k} \qquad \boldsymbol{e}_{pq} = (\boldsymbol{e}^i(p)\cdot \boldsymbol{e}^j(q))_{i,j=1,\dots,d}.$$

Prolongation is defined by

$$\boldsymbol{P}_{k-1}^k = \left(\boldsymbol{R}_k^{k-1}\right)^{\mathrm{T}}.$$

Local obstacles

$$\underline{\boldsymbol{\psi}}^{(k)} = \left(\underline{\boldsymbol{\psi}}_p^{(k)}\right)_{p\in\mathcal{N}_k}, \quad \underline{\boldsymbol{\psi}}_p^{(k)} = \left((\underline{\psi}_p^{(k)})^i\right)_{i=1,\dots,d}, \qquad \overline{\boldsymbol{\psi}}^{(k)} = \left(\overline{\boldsymbol{\psi}}_p^{(k)}\right)_{p\in\mathcal{N}_k}, \quad \overline{\boldsymbol{\psi}}_p^{(k)} = \left((\overline{\psi}_p^{(k)})^i\right)_{i=1,\dots,d}$$

are initialized according to (35). Monotone restriction

$$\underline{\boldsymbol{\psi}}^{(k-1)} = \underline{\mathcal{R}}_k^{k-1}(\underline{\boldsymbol{\psi}}^{(k)}), \qquad \overline{\boldsymbol{\psi}}^{(k-1)} = \overline{\mathcal{R}}_k^{k-1}(\overline{\boldsymbol{\psi}}^{(k)}),$$

is defined according to (36). Local obstacles $\underline{\boldsymbol{\psi}}^{(k)}$, $\overline{\boldsymbol{\psi}}^{(k)}$ give rise to the constraints

$$\boldsymbol{\mathcal{D}}^{(k)} = \{\boldsymbol{v} \in \mathbb{R}^{dn_k} \mid \underline{\boldsymbol{\psi}}^{(k)} \le \mathrm{trc}(\boldsymbol{v}) \le \overline{\boldsymbol{\psi}}^{(k)}\}.$$

For given matrix $\boldsymbol{A}^{(k)} = (\boldsymbol{a}_{pq}^{(k)})_{p,q\in\mathcal{N}_k}$, residual $\boldsymbol{r}^{(k)}$ and constraints $\boldsymbol{\mathcal{D}}^{(k)}$, the approximate correction resulting from one step of projected block Gauß–Seidel relaxation with $d\times d$ blocks $\boldsymbol{a}_{pq}^{(k)}$ is denoted by $GS_k(\boldsymbol{A}^{(k)}, \boldsymbol{r}^{(k)}, \boldsymbol{\mathcal{D}}^{(k)})$. Now we are ready to rewrite our algorithm as a multigrid V–cycle.

Algorithm 1

given: $\boldsymbol{u}_\ell^\nu \in \mathbb{R}^{n_k}$
compute: $\bar{\boldsymbol{u}}_\ell^\nu = \boldsymbol{u}_\ell^\nu + GS_\ell(\boldsymbol{A}, \boldsymbol{r}, \boldsymbol{\mathcal{D}})$ (fine grid smoothing)
initialize:
$\boldsymbol{A}^{(\ell)} = \mathrm{trc}(\boldsymbol{A}) \quad \boldsymbol{r}^{(\ell)} = \mathrm{trc}(\boldsymbol{b} - \boldsymbol{A}\bar{\boldsymbol{u}}_\ell^\nu)$ (truncated stiffness matrix and residual)
$\underline{\boldsymbol{\psi}}^{(\ell)}$, $\overline{\boldsymbol{\psi}}^{(\ell)}$ according to (35) (local obstacles)
for $k = \ell-1, \dots, 1$ do
{
$\boldsymbol{v}^{(k)} = GS_k(\boldsymbol{A}^{(k)}, \boldsymbol{r}^{(k)}, \boldsymbol{\mathcal{D}}^{(k)})$ (projected block Gauß–Seidel smoothing)
$\boldsymbol{r}^{(k)} = \boldsymbol{r}^{(k)} - \boldsymbol{A}^{(k)}\boldsymbol{v}^{(k)}$ (update of residual)
$\underline{\boldsymbol{\psi}}^{(k)} = \underline{\boldsymbol{\psi}}^{(k)} - \boldsymbol{v}^{(k)} \qquad \overline{\boldsymbol{\psi}}^{(k)} = \overline{\boldsymbol{\psi}}^{(k)} - \boldsymbol{v}^{(k)}$ (update of local obstacles cf. (37))
$\boldsymbol{A}^{(k-1)} = \boldsymbol{R}_k^{k-1}\boldsymbol{A}^{(k)}\boldsymbol{P}_{k-1}^k$ (Galerkin restriction of stiffness matrix)
$\boldsymbol{r}^{(k-1)} = \boldsymbol{R}_k^{k-1}\boldsymbol{r}^{(k)}$ (restriction of residual)
$\underline{\boldsymbol{\psi}}^{(k-1)} = \underline{\mathcal{R}}_k^{k-1}(\underline{\boldsymbol{\psi}}^{(k)}), \qquad \overline{\boldsymbol{\psi}}^{(k-1)} = \overline{\mathcal{R}}_k^{k-1}(\overline{\boldsymbol{\psi}}^{(k)})$ (monotone restriction of local obstacles cf. (36))
}
$\boldsymbol{v}^{(0)} = GS_0(\boldsymbol{A}^{(0)}, \boldsymbol{r}^{(0)}, \boldsymbol{\mathcal{D}}^{(0)})$ (approx. solution on $\mathcal{T}_0$)
for $k = 1, \dots, \ell-1$ do
{
$\boldsymbol{v}^{(k)} = \boldsymbol{v}^{(k)} + \boldsymbol{P}_{k-1}^k\boldsymbol{v}^{(k-1)}$ (Interpolation)
}
new iterate: $\boldsymbol{u}_\ell^{\nu+1} = \bar{\boldsymbol{u}}_\ell^\nu + \boldsymbol{P}_{\ell-1}^\ell\boldsymbol{v}^{(\ell-1)}$

Our implementation of Galerkin restriction takes advantage of the fact that local update of the coincidence set only causes local update of the stiffness matrix.

Let us briefly consider some variants of the above multigrid algorithm which can be analyzed in the same general framework and which have convergence properties as stated in Theorem 3.

In order to further improve coarse grid transport in the transient phase, i.e., until the exact coincidence set is known, we consider a *fully truncated variant* performing truncation recursively on all levels in all directions $i = 1, \dots, d$. More precisely, we introduce d different sets of critical nodes $\mathcal{N}_k^{\bullet,i}$, $i = 1, \dots, d$, on each refinement level k. Starting with $\mathcal{N}_\ell^{\bullet,1} = \mathcal{N}_\ell^\bullet(\bar{u}_\ell^\nu)$ and $\mathcal{N}_\ell^{\bullet,i} = \emptyset$, $i = 2, \dots, d$, the update

$$\mathcal{N}_k^{\bullet,i} = (\mathcal{N}_{k+1}^{\bullet,i} \cap \mathcal{N}_k^\bullet) \cup \{p \in \mathcal{N}_k \mid \text{constraint in the direction of } \boldsymbol{e}^i(p) \text{ was activated when computing } v_p^{(k)}\}$$

takes place after correction on level k. Recursive truncation can be formulated algebraically by introducing an operator trc_k that annihilates coefficients associated with i and p, if $p \in \mathcal{N}_k^{\bullet,i}$. Implementation uses appropriate flags. Corresponding quasioptimal local obstacles are obtained by a similar modification of (36). We have already seen that no constraints are active in local coarse grid problems, if the exact coincidence set $\mathcal{N}_j^\bullet(u_j)$ has been detected and coarse grid corrections are small enough. Hence, in the non–degenerate case, fully truncated monotone multigrid still asymptotically reduces to the linear subspace correction generated by (41).

Multiple pre– and postsmoothing or W–cycles are performed in the usual way. In terms of subspace corrections such algorithms can be formulated by multiple occurrence of the same coarse grid space $V_p^{(k)}$.

Exact solution on the initial grid $\mathcal{T}_0$ corresponds to replacing the spaces $V_p^{(0)}$, $p \in \mathcal{N}_0$, by $V^{(0)} = S_0$.

In case of adaptively refined grids, coarse grid smoothing is applied only at new nodes and their neigbours. Again, there is a corresponding interpretation in terms of subspaces $V_p^{(k)}$. In the adaptive case, it may happen that the dimension of $V_p^{(k)}$ is less than d.

Other finite element discretizations like piecewise quadratics or bilinear elements on quadrilaterals can be treated in a similar way. We only have to plug in the appropriate nodal basis functions instead of $\lambda_p^{(k)}$.

6. Hertz Contact Problem

In our first example, we consider a plane strain problem for a half circle centered at $(0, 0.4)$ with radius 0.4 in elastic contact with a rigid plane. The material of the half circle is assumed to be homogeneous and isotropic with Young's modulus $E = 270269$ N/mm^2 and Poisson's ratio $\nu = 0.248$. We prescribe vertical displacement $u(x,y) = -0.005$ at $\Gamma_D = \{(x,y) \in \Gamma \mid y = 0.4\}$ and the Signorini boundary conditions (7) at $\Gamma_C = \partial\Omega \setminus \Gamma_D$. The continuous problem is discretized by linear and bilinear finite elements on triangles and quadrilaterals, respectively. In this example, normals $\boldsymbol{n}_\ell(p) = \boldsymbol{n}(p)$, $p \in \mathcal{N}_\ell$, are chosen to be the outer normal of the plane. An example with varying normals will be given in the next section.

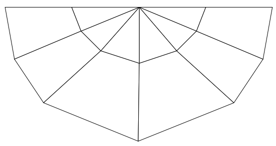

Figure 1. Initial partition $\mathcal{T}_0$

Starting with the initial partition $\mathcal{T}_0$ as depicted in Figure 1 a sequence $\mathcal{T}_0, \dots, \mathcal{T}_\ell$, $\ell = 11$, is produced by adaptive refinement. Local error indicators are provided by an hierarchical a posteriori error estimate in the spirit of [24]. Since Ω is not resolved by the coarse grid, new nodes are moved onto the boundary $\partial\Omega$.

For the iterative solution of the discrete problems we use the fully truncated variant of our monotone multigrid method as described at the end of the preceding section. On each level $k > 0$, we apply 4 pre– and 4 postsmoothing steps. Problems on level 0 are solved up to machine precision by projected block Gauß–Seidel iteration. On subsequent levels $k \ge 1$ the iterate $\tilde{u}_k = u_k^{\nu+1}$ is accepted, if the estimated algebraic error is reduced below 0.05%, i.e., if the stopping criterion

$$\|u_k^{\nu+1} - u_k^\nu\| \le 0.005\, \sigma_{\mathrm{alg}} \sigma_{\mathrm{app}} \|u_k^\nu\|$$

is satisfied with safety parameters $\sigma_{\mathrm{alg}} = 1$, $\sigma_{\mathrm{app}} = 0.1$. As a consequence, the estimated algebraic error does not interfere with the estimated discretization error on the final level (cf. [25], pp. 108). We choose initial iterates $u_k^0 = \tilde{u}_{k-1}$ for $k = 1, \dots, 11$ (nested iteration).

The resulting approximation history is reported in Table 1. It turns out that only 3 iteration steps are required on each refinement level.

The error of displacements is measured in the energy norm. Note that the estimated error is proportional to $n_k^{1/2}$ which is in good agreement with well–known $\mathcal{O}(h)$–estimates.

level	# dof	# iterations	# coincidence set	estimated errors in % displacements	estimated errors in % normal stress
0	30	–	1	64.93	72.12
1	78	3	1	46.68	58.48
2	146	3	1	37.52	33.31
3	222	3	3	18.20	7.54
4	508	3	5	12.52	0.47
5	1 016	3	7	7.51	0.52
6	2 220	3	15	4.77	0.33
7	5 600	3	29	2.91	0.21
8	13 032	3	51	1.92	0.22
9	39 976	3	89	1.10	0.20
10	67 274	3	119	0.84	0.20
11	109 534	3	163	0.65	0.20

TABLE 1. Approximation history

As the final partition $\mathcal{T}_{11}$ is beyond the resolution of printers the deformed partition on level 7 is shown in the left picture of Figure 2. The computed displacements are scaled by a factor of 10 and thus the planar shape of the rigid foundation is not reproduced.

Contact stresses are of primary interest in many applications, (cf. e.g. [1]). Final approximation of tangential and normal boundary stress is depicted in the right picture of Figure 2. We emphasize that tangential stresses are zero up to an algebraic error which could be reduced down to machine precision by sufficiently many multigrid iterations. We now check the accuracy of normal stress. Following [17], see also [22, p. 141], normal contact stresses can be computed analytically from the Hertz solution. Approximating the width of the contact surface of u by the width of the contact surface of the discrete solution u_{11} an approximate Hertzian normal contact stress can be computed analytically. As usual (see e.g. [7, 32]) this approximate Hertzian contact stress is taken as reference solution. The last column of Table 1 contains the relative deviation of maximal normal stress of $\tilde{u}_k$ from maximal Hertzian normal stress. Both coincide up to an error of less than 0.5% for $k = 4$. Note that the coincidence set contains only 5 nodes on this level. Saturation on finer meshes might be due to the fact that Hertzian solution relies on a parabolic instead of a circular shape of Γ_C [33]. The impressive overall accuracy is a consequence of our solution approach which *does not involve any relaxation of contact conditions* in contrast to dual methods or penalty.

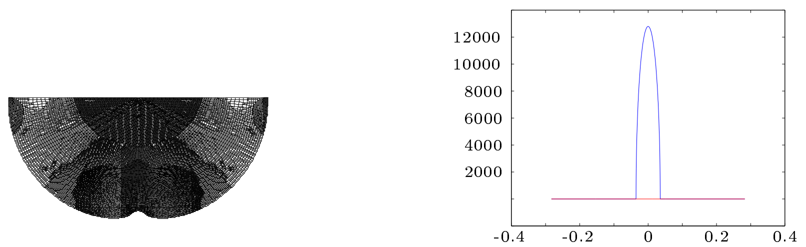

FIGURE 2. Deformed partition $\mathcal{T}_7$ and final approximation of boundary stress at Γ_C

We now investigate the convergence behavior of our multigrid method on the final grid $\mathcal{T}_{11}$. The left picture of Figure 3 shows the algebraic error $\|u_{11} - u_{11}^{\nu}\|$ for $\nu = 0, \dots, 33$. The red curve is obtained using the initial iterate $u_{11}^0 = \tilde{u}_{10}^3$ (nested iteration). We observe linear convergence throughout the iteration. In fact, the exact discrete coincidence set is detected after 1 step. Leading high convergence speed is due to fast reduction of the high frequency contributions of the error. The blue curve illustrates the iteration history for the (artificial) initial iterate $u_{11}^0 = 0$. In this case the discrete coincidence set is detected after 10 iterations. In spite of leading fully nonlinear iterations we again observe a linear reduction of the error throughout the iteration. This effect is not typical but reflects the simplicity of the Hertzian model problem under consideration.

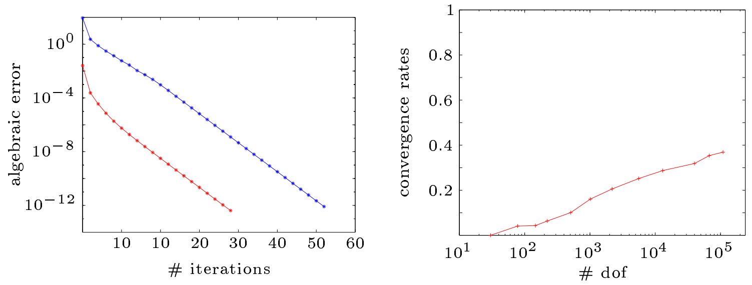

FIGURE 3. Iteration history on level $\ell = 11$ and asymptotic convergence rates

In our final experiment, we compute approximate *asymptotic convergence rates* ρ_k according to

$$\rho_k = \frac{\|u_k^{\nu^*+1} - u_k^{\nu^*}\|}{\|u_k^{\nu^*} - u_k^{\nu^*-1}\|} \tag{44}$$

on each level $k = 0, \dots, 11$. Here, ν^* is chosen such that

$$\|u_k^{\nu^*+1} - u_k^{\nu^*}\| < 10^{-12} \; .$$

As illustrated by the right picture in Figure 3, asymptotic convergence rates seem to saturate at about $\rho_\infty = 0.4$ for increasing levels $k \to \infty$.

7. Elastic cylinder and two rigid rods

We consider the deformation of an elastic cylinder with axis $\{(x, y, z) \,|\, y = 0.5,\ z = 1.0\}$, radius 1 and length 1 against two rigid cylindrical rods with axis $\{(x, y, z) \,|\, x = 0.25,\ z = -0.25\}$ and $\{(x, y, z) \,|\, x = 0.75,\ z = -0.25\}$, respectively, radius 0.25 and infinite length. We choose homogeneous and isotropic material with Young's modulus $E = 206000\ \mathrm{N/mm}^2$ and Poisson's ratio $\nu = 0.28$. Dirichlet boundary conditions $u(x, y) = -0.05$ are prescribed at $\Gamma_D = \{(x, y, z) \in \partial\Omega \mid z \geq 0.75\}$ and Signorini boundary conditions at $\Gamma_C = \{(x, y, z) \in \partial\Omega \mid z \leq 0.25\}$. The remaining part of the boundary is kept stress free.

The continuous problem is discretized by trilinear finite elements on quadrilaterals. The normals $\boldsymbol{n}_\ell(p) = \boldsymbol{n}(p)$, $p \in \mathcal{N}_\ell$, are directed in radial direction of the cylinder. The initial partition $\mathcal{T}_0$ is shown in Figure 4. Again, we produce a sequence $\mathcal{T}_0, \dots, \mathcal{T}_\ell$, $\ell = 5$, by successive local refinement moving new

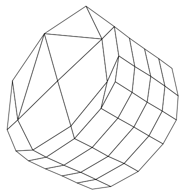

FIGURE 4. Initial partition $\mathcal{T}_0$

nodes at the boundary onto $\partial\Omega$. In order to maximize the significance of the nonlinearity at Γ_C in the discrete problem, only those elements having at least one vertex $p = (p_x, p_y, p_z)$ with $p_z < 0.04$ are refined in each step. Again, we consider the fully truncated monotone multigrid with 4 pre– and 4 postsmoothing steps, and the coarse–grid problems on level 0 are solved up to machine precision.

The deformed final partition $\mathcal{T}_5$ together with the final approximation of contact stress is shown in Figure 5. Recall that the condition $\sigma_T = 0$ is fulfilled up to algebraic accuracy, and that in contrast to penalty methods, the error of the computed boundary stresses depends only on algebraic accuracy and discretization parameters.

The convergence history on the final grid $\mathcal{T}_5$ is shown in the left picture of Figure 6. Again the red curve corresponds to nested iteration. As in the previous example, the resulting initial iterate is sufficiently accurate to enter the asymptotic regime immediately. This is different for the artificial guess $u_5^0 = 0$. As illustrated by the blue curve, it takes about 50 transient steps to reach the asymptotic regime. Note that the asymptotic convergence rates are the same, as predicted by Theorem 2. We

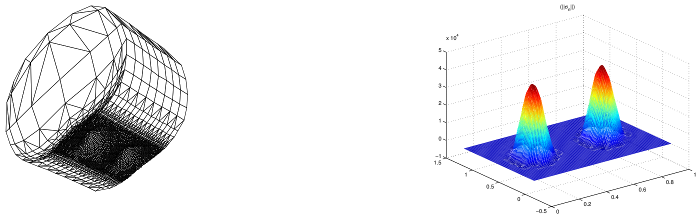

FIGURE 5. Deformed final partition $\mathcal{T}_5$ and final approximation of boundary stress at Γ_C

remark, that it is possible to shorten the initial transient phase by various heuristic strategies, e.g., by additional truncation for very small $(\overline{\psi}_p^{(k)})^i$ or $(\underline{\psi}_p^{(k)})^i$, respectively. Using a W–cycle instead of V–cycle also shortens the transient phase.

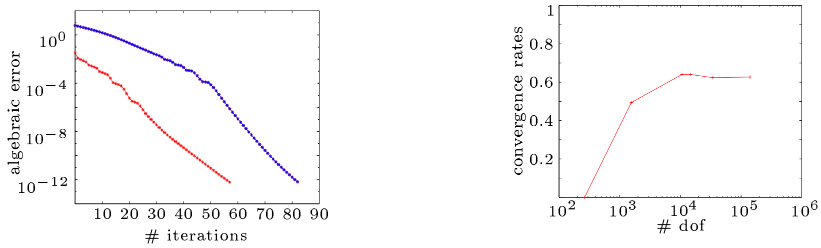

FIGURE 6. Iteration history on level $\ell = 5$ and asymptotic convergence rates

In order to illustrate the convergence behavior for decreasing meshsize, we compute approximate asymptotic convergence rates ρ_k, $k = 0, \ldots, 5$, according to (44). The right picture in Figure 6 indicates that asymptotic convergence rates saturate at about $\rho_\infty = 0.65$ for increasing levels $k \to \infty$. We remark that the asymptotic convergence can be easily accelerated by Krylov–methods such as a conjugate gradient method.

ACKNOWLEDGEMENT. The authors gratefully acknowledge the friendly collaboration with G. Wittum and his group now at IWR Heidelberg, in particular with C. Wieners and P. Bastian. Moreover both authors shared the hospitality of P. Deuflhard in their early days in Berlin.

REFERENCES

[1] M. Ast, H. Rösle, and R. Schenk. FEM–Analyse reibschlüssiger Welle–Naben–Verbindungen. In *Proceedings of the VDI–Fachtagung über Welle–Naben–Verbindungen*, Fulda, 1998.
[2] H. Bader and R.H.W. Hoppe. Multigrid solution of Signorini type problems in contact elastostatics. Technical Report TUM–M9304, TU München, 1993.
[3] P. Bastian, K. Birken, K. Johannsen, S. Lang, N. Neuss, H. Rentz-Reichert, and C. Wieners. UG – a flexible software toolbox for solving partial differential equations. *Computing and Visualization in Science*, 1:27–40, 1997.
[4] V. Belsky. A multi–grid method for variational inequalities in contact problems. *Computing*, 51:293–311, 1993.
[5] D.P. Bertsekas. *Constrained Optimization and Lagrange Multiplier Methods.* Academic Press, New York, 1982.
[6] A. Brandt and C.W. Cryer. Multigrid algorithms for the solution of linear complementary problems arising from free boundary problems. *SIAM J. Sci. Stat. Comput.*, 4:655–684, 1983.
[7] C. Carstensen, O. Scherf, and P. Wriggers. Adaptive finite elements for elastic bodies in contact. *SIAM J. Sci. Comput.*, 20:1605–1626, 1999.
[8] Z. Dostál. Box constrained quadratic programming with proportioning and projections. *SIAM J. Optim.*, 7:871–887, 1997.
[9] M. Dryja and W. Hackbusch. On the nonlinear domain decomposition method. *BIT*, 32:296–311, 1997.
[10] G. Duvaut and J.L. Lions. *Les Inéquations en Mécanique et en Physique.* Dunaud, Paris, 1972.
[11] C. Eck, O. Steinbach, and W. Wendland. A symmetric boundary element method for contact problems with friction. *Math. Comput. Simul.*, 50:43–61, 1999.
[12] E. Gelman and J. Mandel. On multilevel iterative methods for optimization problems. *Math. Prog.*, 48:1–17, 1990.
[13] R. Glowinski. *Numerical Methods for Nonlinear Variational Problems.* Springer, New York, 1984.

[14] R. Glowinski, J.L. Lions, and J.L. Trémolières. *Numerical Analysis of Variational Inequalities.* North–Holland, Amsterdam, 1981.

[15] R. Glowinski and P. Le Tallec. *Augmented Lagrangian and Operator Splitting Methods in Nonlinear Mechanics.* SIAM, Philadelphia, 1989.

[16] W. Hackbusch and H.D. Mittelmann. On multigrid methods for variational inequalities. *Numer. Math.*, 42:65–76, 1983.

[17] H. Hertz. Über die Berührung fester elastischer Körper. *J.f. Math.*, 92, 1882.

[18] R.H.W. Hoppe. Multigrid algorithms for variational inequalities. *SIAM J. Numer. Anal.*, 24:1046–1065, 1987.

[19] R.H.W. Hoppe. Une méthode multigrille pour la solution des problemes d'obstacle. *RAIRO, Modélisation Math. Anal. Numer.*, 24:711–735, 1990.

[20] R.H.W. Hoppe and R. Kornhuber. Adaptive multilevel–methods for obstacle problems. *SIAM J. Numer. Anal.*, 31:301–323, 1994.

[21] J. Nečas I. Hlaváček, J. Haslinger and J. Lovíšek. *Solution of Variational Inequalities in Mechanics.* Springer, Berlin, 1988.

[22] N. Kikuchi and J.T. Oden. *Contact Problems in Elasticity.* SIAM, Philadelphia, 1988.

[23] R. Kornhuber. Monotone multigrid methods for elliptic variational inequalities I. *Numer. Math.*, 69:167–184, 1994.

[24] R. Kornhuber. A posteriori error estimates for elliptic variational inequalities. *Computers Math. Applic.*, 31:49–60, 1996.

[25] R. Kornhuber. *Adaptive Monotone Multigrid Methods for Nonlinear Variational Problems.* Teubner, Stuttgart, 1997.

[26] J. Mandel. A multilevel iterative method for symmetric, positive definite linear complementarity problems. *Appl. Math. Optimization*, 11:77–95, 1984.

[27] J. Schöberl. Efficient contact solvers based on domain decomposition techniques. Technical Report Nr. 545, Universität Linz, 1998.

[28] J. Schöberl. Solving the Signorini problem on the basis of domain decomposition techniques. *Computing*, 60:323–344, 1998.

[29] A. Signorini. Sopra alcune questioni di elastostatica. *Atti della Societá Italiana per il Progresso delle Scienze*, 1933.

[30] X.-C. Tai and J. Xu. Globval convergence of subspace correction methods for convex optimization problems. Submitted to Math. Comp., 1998.

[31] T. Chan W.L. Wan and B. Smith. An energy minimizing interpolation for robust multigrid. Technical Report 98-6, Dept. of Mathematics, UCLA, 1998.

[32] P. Wriggers. Finite element algorithms for contact problems. *Arch. Comp. Meth. Engrg*, 2:1–49, 1995.

[33] P. Wriggers. private communication. 2000.

[34] J. Xu. Iterative methods by space decomposition and subspace correction. *SIAM Review*, 34:581–613, 1992.